Int. J. Electrochem. Sci., 4 **(2009)** 1329 - 1338

International Journal of ELECTROCHEMICAL SCIENCE
www.electrochemsci.org

Electrocatalytic Oxidation of Methanol at γ-MnOOH Nanorods Modified Pt Electrodes

Mohamed S. El-Deab[*]

Department of Chemistry, Faculty of Science, Cairo University, Cairo, Egypt
[*]E-mail: msaada68@yahoo.com

Received: 18 June 2009 / *Accepted:* 15 September 2009 / *Published:* 30 September 2009

The current study addresses the electro-oxidation of methanol in 0.1 M NaOH at Pt electrodes modified with electrodeposited manganese oxide nanorods. Morphological and phase characterizations were performed by SEM, TEM and XRD techniques, respectively, and revealed the electrodeposition of manganese oxide in nanorod morphology with a highly crystalline nature (γ-MnOOH). A significant enhancement of methanol oxidation has been observed at the nano-MnOOH/Pt electrodes as evident from the increase of the oxidation peak current (I_p). The enhancement factor and I_p for methanol electro-oxidation depends on the surface coverage of MnOOH indicating its essential role in the oxidation process of methanol with an optimum surface coverage of ca. 30% under the present experimental conditions. The MnOOH nanorods are believed to act as a catalytic mediator that enhances the electro-oxidation of methanol by facilitating the oxygen supply through a reversible redox system of Mn(III)/(IV) oxides**.**

Keywords: Nanoparticles; Electrocatalysis; γ-MnOOH; Methanol oxidation; Modified electrodes.

1. INTRODUCTION

Methanol oxidation reaction (MOR) is one of the most extensively studied reactions. It is a vital anodic reaction in direct methanol fuel cells (DMFC) which are considered a promising system for providing the increasing demand for energy [1,2]. Methanol, as a liquid fuel, is easily transported and stored in comparison to hydrogen gas. Electro-oxidation of methanol is a vital anodic process in DMFC. However, this anodic process suffers from several difficulties, including the generation of various reaction intermediates which cause the deactivation of the anode. Thus, the search for new and efficient electrocatalysts is a major challenge in the development and commercialization of fuel cells, i.e., increasing the anode tolerance against the reaction intermediates particularly of carbon monoxide (CO).

So far, Pt is considered a necessary component for the fabrication of active catalysts for the electro-oxidation of methanol. It provides a suitable base for methanol adsorption and it effectively catalyzes the dehydrogenation step [3,4]. However, the complete oxidation of methanol to CO_2 requires the availability of oxygen at low potentials. Thus, Pt alone is not sufficient to catalyze the reaction at a reasonable rate, mainly because of the surface poisoning by the adsorption of several incompletely oxidized carboneous intermediates (i.e., methanol residues, e.g., CO). The latter species block the active surface sites of Pt and thus impede the adsorption of methanol. This causes a significant deterioration of the performance of Pt towards electro-oxidation of methanol. In this context, several modifications of Pt-based electrocatalysts have been suggested for the electro-oxidation of methanol with an aim to mitigate such poisoning effects [3-23]. These include Pt-Ru [3,5-11], Pt-Pb [12] in addition to metallic and/or metal oxide-based Sb-Sn, Co-Mn, Ni-Si, Ni-Cr-Mo, Fe-Cr [13-19], MnO_x/Ru and MnO_2/Pt catalysts [20,21].

This study addresses an alternative way of modifying Pt surface by the electrodeposition of crystallographically-oriented manganese oxide nanorods (in the manganite phase, γ-MnOOH [24]). This was done, in a trial to increase the CO tolerance and to improve the performance of the Pt electrode, with the expectation of obtaining an effective catalyst with high electrocatalytic activity towards oxidation of methanol in alkaline medium. γ-MnOOH nanorods are believed to provide oxygen species to adsorbed intermediates and thus enhance CO oxidation to CO_2 at low potential.

2. EXPERIMENTAL PART

2.1. Electrodes

The working electrode was a polycrystalline Pt wire (d = 2.0 mm) sealed in a Teflon jacket. The exposed geometric surface area of the electrode was 3.14 x 10^{-2} cm^2, having a roughness factor of 3.55 (calculated from the charge consumed during the reduction of the surface oxide monolayer -peak located at ca. 0.4 V vs. SCE, c.f. Fig. 3- formed during the anodic potential scan using a reported value of 420 μC cm^{-2} [25]). A SCE and a spiral Pt wire were used as the reference and counter electrodes, respectively. The Pt electrode was mechanically polished with aqueous slurries of successively finer alumina powder (down to 0.05 μm) and was sonicated for 10 min in Milli-Q water, then was electrochemically pretreated in N_2-saturated 0.1 M H_2SO_4 solution by cycling the potential between –0.3 and 1.25 V vs. SCE at 50 mV s^{-1} for 10 min or until a reproducible CV characteristic for a clean poly-Pt electrode was obtained (cf. Fig. 3a).

2.2. Deposition of manganese oxide

Manganese oxide nanorods (referred hereafter as nano-MnOx) were electrodeposited on the surface of the thus-pretreated Pt electrode from an aqueous solution of 0.1 M Na_2SO_4 containing 0.1 M $Mn(CH_3COO)_2$ by cycling the potential between –50 and 350 mV vs. SCE at 20 mV s^{-1} several times

[26,27]. The surface coverage of the nano-MnOx has been controlled by the number of potential cycles employed during the electrodeposition step (cf. Table 1).

2.3. Characterization

Electrochemical characterization of the nano-MnOx modified Pt electrodes has been achieved by measuring the characteristic CVs in N_2-saturated 0.1 M H_2SO_4 (cf. Fig. 3b as an example) from which the real surface area of the unmodified and nano-MnOx modified Pt electrodes were estimated [25]. Table 1 lists the value of surface coverage of nano-MnOx at various number of potentials cycles. The morphological characterization of the prepared catalysts (i.e., MnOx/Pt) was depicted by scanning electron microscopy (SEM) using a JSM-T220 (JEOL, Optical Laboratory, Japan) at an acceleration voltage of 12 kV and a working distance of 4-5 mm, and transmission electron microscope (TEM) using a JEM-2010F (JEOL, Optical Laboratory, Japan) at a working voltage of 200 kV. While the crystallographic structure of the MnOx was examined with X-ray diffraction (XRD) technique using a Philips PW 1700 powder X-ray diffractometer with a Ni-filtered Cu $K\alpha_1$ radiation (λ = 1.54056 Å) working at 40 kV and 30 mA.

2.4. Electrochemical measurements

The electrocatalytic activity of the nano-MnOx modified Pt electrodes towards electro-oxidation of methanol was examined in a deaerated aqueous solution of 0.1 M NaOH solution containing 0.3 M methanol. CV measurements were performed in a conventional two-compartment glass cell. All chemicals (analytical grade) were used as received without further purification. All measurements were performed at room temperature (25 ± 1^{o}C). All current densities were calculated on the basis of the geometric surface area of the working electrode.

3. RESULTS AND DISCUSSION

3.1. Characterization of MnOx

Fig. 1A shows a typical SEM micrograph obtained for nano-MnOx/Pt electrodes. The MnOx was electrodeposited onto the Pt electrode by applying 50 potential cycles. This figure shows that MnOx is deposited in a porous texture composed of intersectioned nanorods (with average width of ca. 20 nm) onto the Pt electrode. This texture covers homogeneously the entire surface of the electrode in a rather porous texture enabling the access of the solution species to the underlying Pt substrate through nano channels across the MnOx texture. Transmission electron microscope (TEM) image (Fig. 1B) of the MnOx electrodeposited onto Pt screen (grade size = 2000 mesh) indicates the growth of the MnOx nanorods without any significant branching or formation of dendrite.

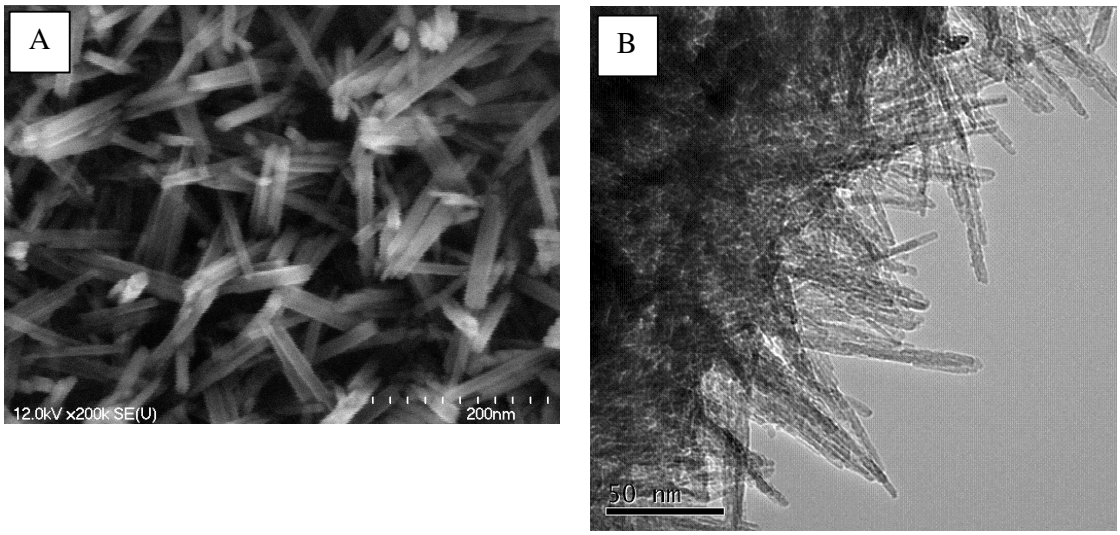

Figure 1. (A) SEM and (B) TEM images of nano-MnOx modified Pt electrodes. Manganese oxide nanorods were electrodeposited onto (A) planar Pt electrode and (B) Pt screen of 2000 mesh by applying 50 potential cycles.

Fig. 2 shows XRD pattern of nano-MnOx electrodeposited onto Pt substrate (curve b) by applying 50 potential cycles. XRD pattern of bare Pt substrate is shown for comparison (curve a). Inspection of this figure reveals the existence of three peaks at 2θ of ca. 39, 46 and 67°, corresponding, respectively, to Pt(111), Pt(200) and Pt(220) facets of the polycrystalline Pt (curves a and b). Additionally, a new peak is observed at 2θ of ca. 26.5° upon the electrodeposition of manganese oxide (see curve b). This peak is perfectly indexed to the $(11\bar{1})$ crystallographic plane of monoclinic manganese oxide in gamma phase (γ-MnOOH) [24,28,29].

Fig. 3 shows CVs measured in 0.1 M H_2SO_4 for (a) bare Pt and (b) nano-MnOx/Pt electrodes prepared by applying 15 potential cycles. Potential scan rate: 50 mV s^{-1}. This figure reveals a decrease of the peak current intensity around 0.4 V (corresponding to the reduction of the Pt surface oxide monolayer formed during the anodic scan). This indicates the effective electrodeposition of nano-MnOx onto the Pt surface. The decrease in the intensity of this peak is used as a probing index of the extent of MnOx surface coverage onto Pt surface (cf. Table 1).

3.2. Methanol oxidation

The thus-prepared nano-MnOx/Pt electrodes with various surface coverages were tested for their electrocatalytic activity for methanol oxidation. Fig. 4 shows a typical example of CVs for (a) bare Pt and (b) nano-MnOx/Pt (surface coverage ≈ 30%) electrodes measured in N_2-saturated 0.1 M NaOH solution containing 0.3 M methanol. This figure shows that the modification of Pt with a submonolayer of MnOx causes a little shift in the onset oxidation of methanol to less positive potential

concurrently with a significant increase in the peak current (I_p). This catalytic enhancement points to a crucial role of nano-MnOx in the oxidation process of methanol.

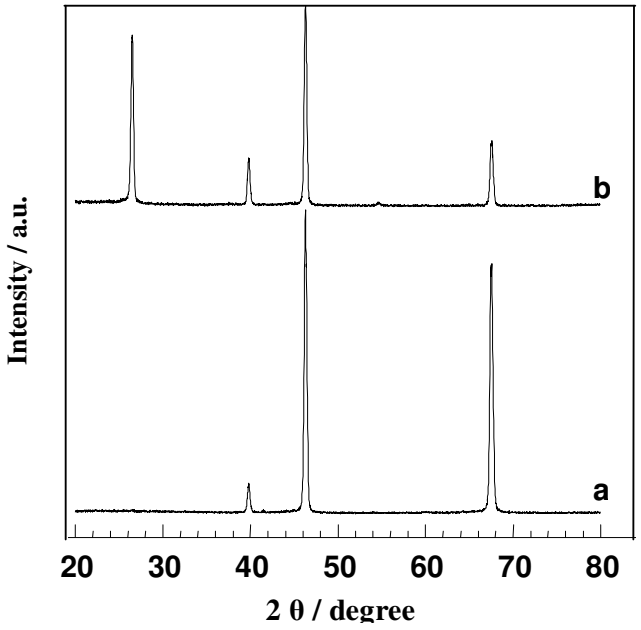

Figure 2. XRD patterns of (a) bare (i.e., unmodified) and (b) nano-MnOx modified Pt electrodes. Manganese oxide nanorods were electrodeposited by applying 50 potential cycles.

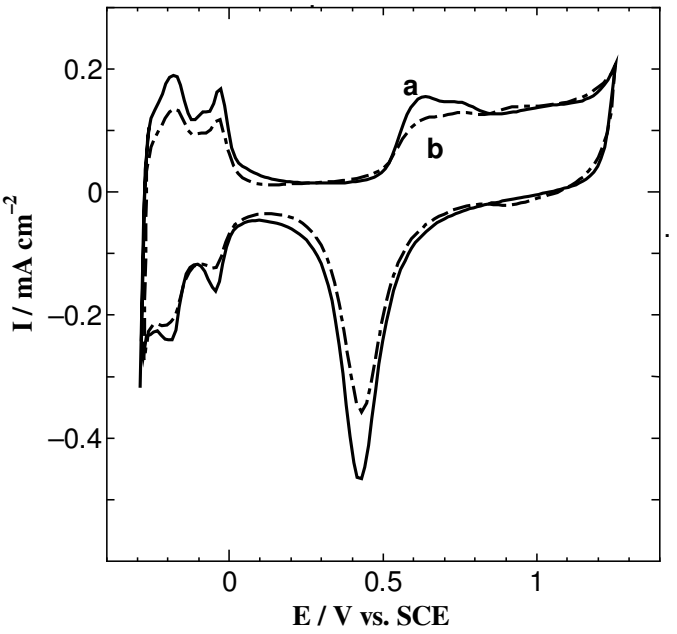

Figure 3. CVs measured in N_2-saturated 0.1 M H_2SO_4 for (a) bare and (b) nano-MnOx modified Pt electrodes (surface coverage ≈ 20%). Potential scan rate: 50 mV s^{-1}. MnOx nanorods were electrodeposited onto Pt electrode by applying 15 potential cycles.

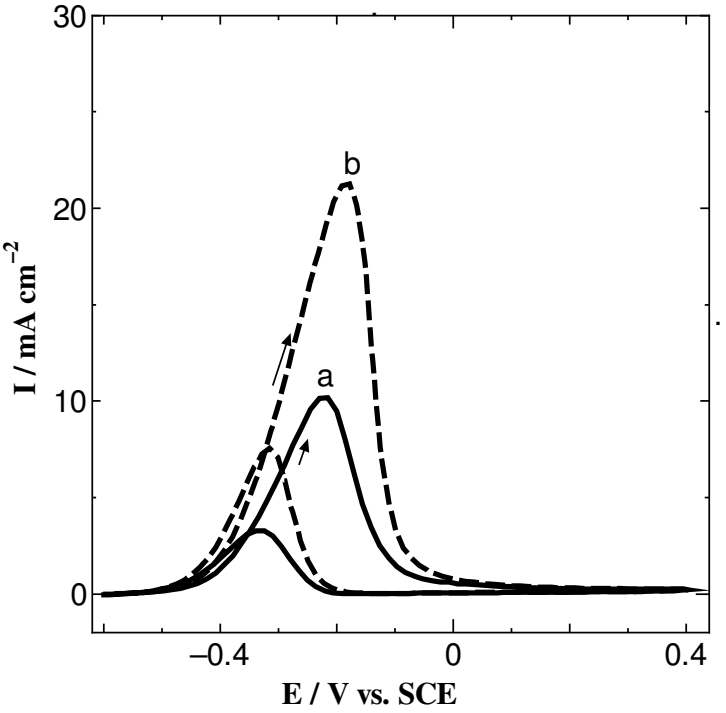

Figure 4. CVs for methanol electro-oxidation at (a) bare and (b) nano-MnOx modified Pt (surface coverage ≈ 30 %) electrodes in N_2-saturated 0.1 M NaOH containing 0.3 M methanol. Potential scan rate: 50 mV s^{-1}.

Table 1 lists the catalytic enhancement factor (ratio of oxidation currents with and without MnOx on Pt) together with the peak current densities for methanol oxidation as a function of surface coverage of nano-MnOx. This table shows that the catalytic enhancement factor increases with the surface coverage of nano-MnOx with an optimum value around 30%. At higher MnOx coverages I_p decreases probably due to the blocking of the Pt active sites with the excessive amount of nano-MnOx.

Table 1. Variation of the catalytic enhancement factor for methanol electro-oxidation with surface coverage of MnOx on Pt electrodes in 0.1 M NaOH + 0.3 M methanol.

Nano-MnOx loading (no. of potential cycles)	Surface coverage [a] / %	Enhancement factor [b]	I_p / mA cm^{-2}
0	---	---	10.2
5	11	1.4	14.8
15	21	1.6	16.2
25	30	2.1	21.8
50	45	1.1	11.3

[a] *Estimated from the decrease in the charge consumed during the reduction of the surface Pt-surface oxide monolayer (formed during the anodic scan) as a result of the electrodeposition of nano-MnOx (peak at ca. 0.4 V vs. SCE, see Fig. 3) using a reported value of 420 μC cm^{-2} [25].*

[b] *Ratio of oxidation currents with and without nano-MnOx on Pt electrodes.*

The stability of nano-MnOx/Pt electrode is tested by recording the current transients (*I-t* curves, Fig. 5A) for methanol oxidation at −250 mV vs SCE at (a) bare Pt and (b) nano-MnOx/Pt (surface coverage ≈ 30%) electrodes. The *I-t* curves show that nano-MnOx/Pt (curve b) supports higher oxidation currents than bare Pt (curve a). Furthermore, CV measurements show that the catalytic activity of the nano-MnOx modified Pt electrode towards methanol oxidation remains effectively unchanged upon the repetitive cycling of the potential up to 100 cycles (Fig. 5B). This demonstrates the preferred oxidation of methanol at the modified electrode and its high tolerance against the poisoning effect of the incompletely oxidized adsorbed intermediates species (e.g., CO) compared to the unmodified Pt. The gradual lose of catalytic activity (albeit small) with time might be attributed to the accumulation of adsorbed intermediates at some Pt active sites which are not reachable by nano-MnOx. This calls for further studies regarding the homogenization of the nano-MnOx deposition atop the Pt surface, which is the task of future investigation.

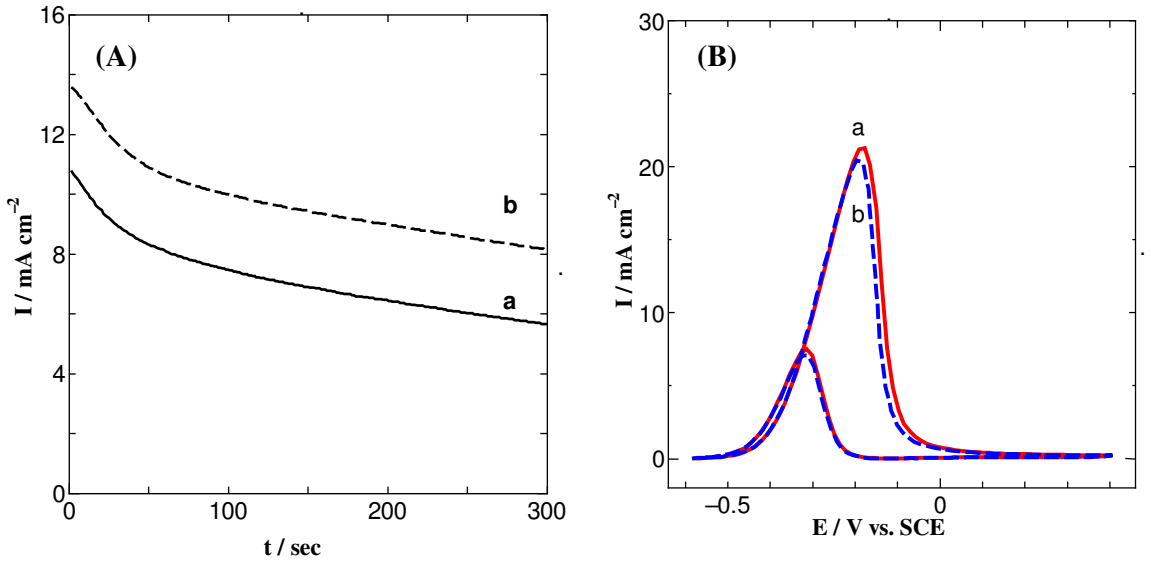

Figure 5. (A) Current transients recorded at −250 mV vs. SCE for methanol oxidation in N_2-saturated 0.1 M NaOH containing 0.3 M methanol at (a) bare and (b) nano-MnOx modified Pt (surface coverage ≈ 30 %) electrodes. (B) First (solid line, trace a) and 100th (dashed line, trace b) CV for methanol oxidation at nano-MnOx/Pt electrodes (surface coverage ≈ 30%) in 0.1 M NaOH + 0.3 M methanol. Potential scan rate: 50 mV s^{-1}.

The origin of the enhanced activity of the modified platinum electrodes has long been attributed to one or a combination of several reasons. The first factor is attributed to an electronic effect of the modifier (e.g., second metal ad-atom) on the underlying platinum leading to favorable adsorption properties of platinum. The second factor is attributed to the bi-functional theory of electrocatalysis in which the second metal is more oxidizable (i.e., with high affinity for the adsorption of oxygen-containing species from solution) than Pt. It thus increases the oxidation rate of the adsorbed intermediates methanol residues (e.g., CO) through a surface reaction. The third factor for the observed enhancement is frequently assigned to a decrease of the electrode poisoning by preventing the formation of a strongly bound intermediate (e.g., CO) [12]. For the current case, XPS studies of the

nano-MnOx/Pt surface revealed the absence of electronic interaction between the electrodeposited manganese oxide and the underlying Pt substrate [24]. Thus, the enhancement of the electrocatalytic performance by nano-MnOx loading does not originate from a change in the electronic properties of the Pt surface atoms. Alternatively, it is reported that oxides (e.g., IrO_2) in which a higher oxidation state is available close to the thermodynamic potential of the anodic oxygen evolution reaction (OER) are excellent candidates anodes for water electrolysis [30,31]. Consistently, nickel oxide in the β-phase (i.e., NiOOH) is shown to enhance the oxidation of small organic molecules as well as the OER [2,3,32] via facilitating the charge transfer and/or oxygen supply at low potentials compared to the unmodified surface. In the current study, the electrodeposited manganese oxide (γ-MnOOH) is likely to function similarly towards the oxidation of methanol in alkaline media due to: (i) its isomorphous structure to NiOOH and (ii) its feasible transformation to the higher oxide (i.e., MnO_2) under the prevailing conditions of potential and pH [30]. The porous texture of nano-MnOx allows methanol molecules to reach the Pt active surface sites and undergo the oxidation process. It is then presumed that nano-MnOx acts as oxygen supplier to the adsorbed intermediates (i.e., methanol residues) facilitating its oxidation to CO_2.

Fig. 6 shows CV measured for nano-MnOx/Pt electrode (with coverage of ca. 30%) in a deaerated methanol-free 0.1 M NaOH. The oxidation peak observed at ca. −320 mV is attributed to the surface reversible oxidation (forward scan)-reduction (reverse scan) reaction of MnOOH to MnO_2 through a mechanism involving proton exchange with the solution according to [27,30,31,33]:

$$MnOOH + OH^- \leftrightarrow MnO_2 + H_2O + e^- \quad (1)$$

MnO_2 (with a strong oxidizing power) is thought to provide oxygen and thus facilitates the oxidation of adjacent carboneous intermediates, e.g., CO (adsorbed at the nearby Pt active sites) to CO_2, leading to retrieval of the Pt active sites (via removal of the poison) as:

$$MnO_2 + Pt\text{-}CO_{ads} + OH^- \rightarrow MnOOH + CO_2 + Pt_{free} + e^- \quad (2)$$

where the term "$Pt\text{-}CO_{ads}$" refers to Pt active surface site blocked with adsorbed CO. The sequential coupling of Reactions 1 and 2 results, effectively, in the generation of CO_2 and retrieval of free Pt active surface sites as:

$$Pt\text{-}CO_{ads} + 2\ OH^- \rightarrow CO_2 + Pt_{free} + H_2O + 2e^- \quad (3)$$

Reaction 2 indicates the regeneration of the γ-MnOOH phase which is believed to act as a catalytic mediator facilitating the oxidation of CO into CO_2. This might furnish a plausible explanation for the observed enhancement of the electro-oxidation of methanol (via the oxidative removal of CO). Similar enhancing effect was observed towards the electro-oxidation of formic acid at nano-MnOx modified planar [34] and nanohole-array type Pt electrodes [35]. Further studies are underway to confirm the enhancing role of γ-MnOOH towards the oxidation of CO at nano-MnOx modified electrode (data will

be reported shortly [36]). Our preliminary results show a significant enhancing effect of CO oxidation at nano-MnOx/Pt compared to the unmodified Pt.

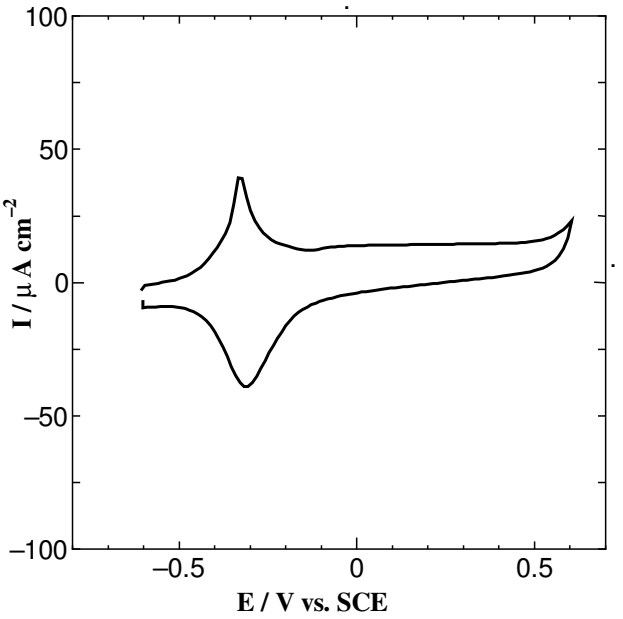

Figure 6. CV for nano-MnOx/Pt electrode in N_2-saturated methanol-free 0.1 M NaOH. Potential scan rate: 50 mV s^{-1}.

4. CONCLUSIONS

The current study introduces a novel metal oxide modified Pt anodes for the electro-catalytic oxidation of methanol in alkaline medium. The electrodeposition of crystallographically oriented manganese oxide nanorods (γ-MnOOH) resulted in a significant enhancement of methanol oxidation as evident from the increase in the anodic peak current. The surface reversible oxidation of MnOOH to MnO_2 is believed to provide oxygen to the adsorbed methanol residues (e.g., CO) thus facilitating its oxidation to CO_2 and leads eventually to the retrieval of the Pt active surface site.

References

1. J. M. Feliu and E. Herrero, in: W. Vielstich, H. A. Gasteiger and A. Lamm (Eds.), *Handbook of Fuel Cells*, Vol. 2, Wiley, New York, 2003.
2. M. A. Abdel Rahim, R. M. Abdel Hameed and M. W. Khalil, *J. Power Sources*, 135 (2004) 42.
3. A. A. Al-Shafei, R. Hoyer, L. A. Kibler and D. M. Kolb, *J. Electrochem. Soc.*, 151 (2004) F141.
4. N. S.-Alvarez, L. R. Alden, E. Rus, H. Wang, F. J. DiSalvo and H. D. Abruna, *J. Electroanal. Chem.*, 626 (2009) 14.
5. J. O'M. Bockris and H. Wroblowa, *J. Electroanal. Chem.*, 7 (1964) 428.

6. H. Binder, A. Kohling and G. Sanstede, *From Electrocatalysis to Fuel Cells*, G. Sanstede (Ed.), University of Washington, Seattle, 1972.
7. H. A. Gasteiger, N. M. Markovic, P. N. Ross and E. J. Cairns, *J. Phys. Chem.*, 98 (1994) 617.
8. H. Nonaka and Y. Matsumura, *J. Electroanal. Chem.*, 520 (2002) 101.
9. S. Lj. Gojkovic, T. R. Vidakovic and D. R. Durovic, *Electrochim. Acta*, 48 (2003) 3607.
10. Z. Jusys, J. Kaiser and R. J. Behm, *Electrochim. Acta*, 47 (2002) 3693.
11. A. O. Neto, R. W. R. V.-Silva, M. Linardi and E. V. Spinacé, *Int. J. Electrochem. Sci.*, 4 (2009) 954.
12. B. Beden, F. Kadirgan, C. Lamy and J. M. Leger, *J. Electroanal. Chem.*, 127 (1981) 75 and the references cited therein.
13. M. C. Pham, F. Adami, P. C. Lacase, J. P. Doucet and J. E. Dubois, *J. Electroanal. Chem.*, 201 (1986) 413.
14. M. Fleischmann, K. Korinek and D. Pletcher, *J. Electroanal. Chem.*, 31 (1971) 39.
15. L. Zhang and D. Xia, *Appl. Surf. Sci.*, 252 (2006) 2191.
16. D. R. Blasini, D. Rochefort, E. fachini, L. R. Alden, F. J. DiSalvo, C. R. Cabrera and H. D. Abruna, *Surf. Sci.*, 600 (2006) 2670.
17. A. N. Sofronkov, *Ukr. Khim. Zh.*, 47 (1981) 15.
18. S. M. Lin and T. C. Wen, *J. Appl. Electrochem.*, 25 (1995) 73.
19. A. A. Al-Shafei, *J. Electroanal. Chem.*, 471 (1999) 89.
20. J. S. Rebello, P. V. Samant, J. L. Figueiredo and J. B. Fernandes, *J. Power Sources*, 153 (2006) 36.
21. G.-Y. Zhao and H.-L. Li, *Appl. Surf. Sci.*, 254 (2008) 3232.
22. A. A. Hathoot, M. Abdel-Kader and M. Abdel-Azzem, *Int. J. Electrochem. Sci.*, 4 (2009) 208.
23. C. Xu, Y. Liu and D. Zuan, *Int. J. Electrochem. Sci.*, 2 (2007) 674.
24. M. S. El-Deab and T. Ohsaka, *Angew. Chem. Int. Ed.*, 45 (2006) 5963.
25. S. Trasatti and O. A. Petrii, *Pure Appl. Chem.*, 63 (1991) 711.
26. M.-S. Wu and P.-C.J. Chiang, *Electrochem. Solid-State Lett.*, 7 (2004) A123.
27. M. S. El-Deab and T. Ohsaka, *J. Electrochem. Soc.*, 155 (2008) D14.
28. Powder Diffraction File, W. F. McClune, Editor, *International Center for Diffraction Data* (ICDD), USA, 2003.
29. R. Yang, Z. Wang, L. Dai and L. Chen, *Mater. Chem. Phys.*, 93 (2005) 149.
30. M. Pourbaix, in *Atlas of Electrochemical Equilibria in Aqeous Solutions*, Pergamon Press, Oxford, 1966, p. 286.
31. S. Fierro, T. Nagel, H. Baltruschat and C. Comminellis, *Electrochem. Commun.*, 9 (2007) 1969.
32. A. M. Fundo and L. M. Abrantes, *Russ. J. Electrochem.*, 42 (2006) 1291
33. S. Ardizzone and S. Trasatti, *Adv. Colloid Interface Sci.*, 64 (1996) 173.
34. M. S. El-Deab, L. A. Kibler and D. M. Kolb, *Electrochem. Commun.*, 11 (2009) 776.
35. M. S. El-Deab, *J. Adv. Research* (2009) in press.
36. M. S. El-Deab and D. M. Kolb, in preparation.